

Optimal control of an 8-DOF vehicle active suspension system using Kalman observer

S. Hossein Sadati, Salar Malekzadeh* and Masood Ghasemi

Department of Mechanical Engineering, K.N.Toosi University of Technology, 4th Tehranpars square, Tehran, Iran

Received 6 December 2006

Abstract. In this paper, an 8-DOF model including driver seat dynamics, subjected to random road disturbances is used in order to investigate the advantage of active over conventional passive suspension system. Force actuators are mounted parallel to the body suspensions and the driver seat suspension. An optimal control approach is taken in the active suspension used in the vehicle. The performance index for the optimal control design is a quantification of both ride comfort and road handling. To simulate the real road profile condition, stochastic inputs are applied. Due to practical limitations, not all the states of the system required for the state-feedback controller are measurable, and hence must be estimated with an observer. In this paper, to have the best estimation, an optimal Kalman observer is used. The simulation results indicate that an optimal observer-based controller causes both excellent ride comfort and road handling characteristics.

Keywords: Active suspension system, 8-DOF model, optimal control, passenger dynamics, ride comfort, Kalman observer, road disturbance

1. Introduction

Demands for better ride comfort and controllability of road vehicle motivate many automotive industries to consider the use of active suspension. The active suspension system made it possible to surpass the compromise between ride comfort and vehicle stability, which was not possible with passive suspension [9]. The idea of active suspension is to insert a force actuator between the sprung and unsprung masses in addition to the spring and the damper, replacing the damper or replacing both spring and the damper. The advantage of the active suspension is due to its capability to control the attitude of the vehicle, to reduce the effects of braking and to reduce the vehicle roll during cornering maneuvers in addition to increase the ride comfort and vehicle road handling.

The actuator is secured in parallel with a spring and shock absorber. Active suspension requires sensors to be located at different points of the vehicle to measure the motions of the body, suspension system and/or the unsprung mass. This information is used in the online controller to command the actuators in order to provide the exact amount of force required [2,3,7].

In any vehicle suspension system, there are a variety of performance parameters which need to be optimized. These parameters include, among others, four important quantities which should be considered carefully in designing a suspension system: ride comfort, body motion, road handling, and suspension travel. The trade-off between ride comfort and road handling characteristics is usually a trial and error procedure. Moreover, no suspension system can simultaneously minimize all four of the above mentioned parameters. The advantage of controlled suspension is that a better set of design trade off is possible rather than with passive systems. Linear optimal control theory provides a systematic approach to design the active suspension controller [5].

In this study, we intend to emphasize the effective methodology of controller design in order to satisfy a preassigned set of design criteria.

*Corresponding author. Tel.: +98 911 3329757; Fax: +98 21 8882997; E-mail: s. malekzadeh@sina.kntu.ac.ir.

This paper is arranged as follows: the full 8-DOF model of a vehicle, including passenger dynamics, is first presented followed by a discussion of the proposed control strategy. A simulation is then made in order to apply the proposed control on the system. Hence, we continue with an exposition of an 8-DOF model of a vehicle including passenger dynamics.

This paper illustrates the importance of passenger dynamics when the objective would be to improve the passenger ride comfort as well as to satisfy the road handling requirements.

2. Mathematical modeling

Mathematical modeling of vehicle, including the passenger dynamics and road disturbance is presented in this section. A linear model is considered to represent the vehicle-passenger dynamics, while a normal random profile is used to model the road roughness.

2.1. Vehicle-passenger model

The dynamical 8 degrees of freedom model of the vehicle with a driver is presented in Fig. 1. The model consists of a body (sprung mass), connected by the suspension systems to four wheels (unsprung masses) and a passenger. Body motions are considered to be bounce, roll, and pitch with every wheel having its own bounce. The passenger is considered to have only vertical oscillations. The suspension, tires and passenger seat are modelled by linear springs in parallel to viscous dampers. The system variable notations with their corresponding values are presented in the nomenclatures at the end of the paper.

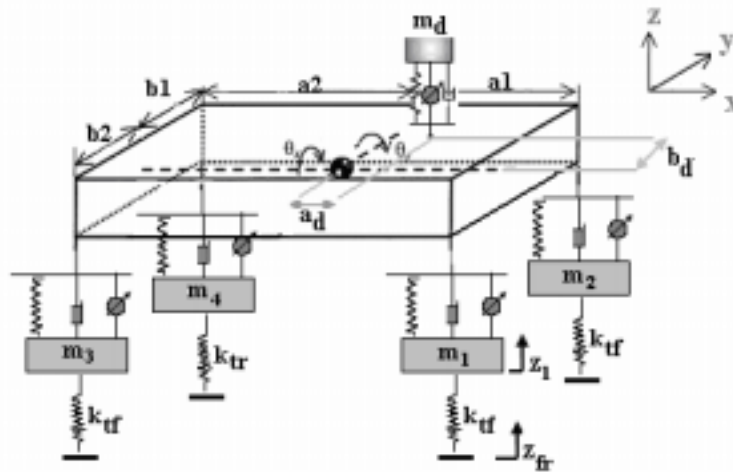


Fig. 1. Linear model of vehicle, passenger and road with 8 degrees of freedom.

The values given for the different variables and parameters in the nomenclature are related to a real Samand vehicle. This vehicle is considered as the “National Vehicle of Iran” whose manufacture began around 2003.

The parameters related to the tires are denoted with subscript t, while the passenger parameters have subscript d. The eight degrees of freedom are: front right wheel displacement, z_1 ; front left wheel displacement, z_2 ; rear left wheel displacement, z_3 ; rear right wheel displacement, z_4 ; body bounce, z_b ; body roll, θ_r ; body pitch, θ_p and passenger bounce, z_d [1].

The actuators are considered to be a source of controllable force, and located in parallel to the suspension spring and shock absorber, passenger seat suspension.

The equation of motion are linear and can be written in matrix form as [12]

$$\dot{x} = Ax + Bu + Gw \quad (1)$$

where the state vector x is defined as

$$x = [z_1 \ z_2 \ z_3 \ z_4 \ z_b \ \theta_p \ \theta_r \ z_d \ \dot{z}_1 \ \dot{z}_2 \ \dot{z}_3 \ \dot{z}_4 \ \dot{z}_b \ \dot{\theta}_p \ \dot{\theta}_r \ \dot{z}_d]^T \quad (2)$$

The input vector u represents the five actuator forces, while the disturbance vector w consists of road disturbances.

$$u = [u_1 \ u_2 \ u_3 \ u_4 \ u_5]^T \quad (3)$$

$$w = [z_{fr} \ z_{fl} \ z_{rl} \ z_{rr}]^T \quad (4)$$

The matrix representation of Eq. (1) would be the basis for the linear optimal controller design.

2.2. Road profile model

In the early days of studying the performance of vehicles on rough roads, functions such as sine waves, step functions or triangular waves were generally applied as disturbances from the ground. While these inputs provide a basic idea for comparative evaluation of designs, it is recognized that the road surface is usually not represented by these simple functions, and therefore the deterministic irregular shapes cannot serve as a valid actual road disturbance for studying the true behavior of the vehicle.

In this paper, a real road surface taken as a random exciting function, is used as the input to the vehicle-road model. Power spectral density (PSD) analysis is used to describe the basic properties of random data. Several attempts have been made to classify the roughness of a road surface. In this study, classifications are based on the international organization for standardization(ISO). The ISO has proposed road roughness classification using the PSD values(ISO, 1982).

Table 1 illustrates the stochastic characteristics of the final random input design, which corresponds to the poor road condition as being classified by ISO.

| Min(m) | Max(m) | PSD($m^3/cycle$) |
|--------|--------|--------------------|
| -0.029 | 0.029 | 0.0004 |

3. Optimal controller design

The performance characteristics which are of most interest when designing the vehicle suspension are passenger ride comfort, body motion, suspension travel and road handling [5].

The linear time-invariant system (LTI) is described by Eq. (1). To design the controller, it is assumed that all the states are available and that they can be measured exactly. First, let us consider a state variable feedback regulator of the type

$$u = -k x \quad (5)$$

where k is the state feedback gain matrix. The optimization procedure consists of determining the control input u , which minimizes the performance index. The performance index J represents the performance characteristic requirement as well as the controller input limitations.

In the conventional method, the performance index J penalizes the state variables and the inputs, thus it has the standard form of

$$J = \int_0^{\infty} (x^T Q x + u^T R u) dt \quad (6)$$

where Q and R are positive definite, known as the weighting matrices.

Using linear optimal control theory [11] for the controller design, the performance index can be written as a weighted sum of the mean square values of output performance variables, including suspension relative travel, passenger relative bounce, passenger acceleration, and body pitch [6]. The passenger acceleration is used here as an indicator of ride comfort. The controller should minimize all the quantities.

The performance index written in terms of the variables used in this study can be written as

$$J = \int_0^{\infty} [q_1(z_{b1} - z_1)^2 + q_2(z_{b2} - z_2)^2 + q_3(z_{b3} - z_3)^2 + q_4(z_{b4} - z_4)^2 + q_5(z_d - z_{b5})^2 + q_6\theta_p^2 + q_7.\ddot{z}_d^2] dt \quad (7)$$

where $(z_{b1} - z_1)$, $(z_{b2} - z_2)$, $(z_{b3} - z_3)$ and $(z_{b4} - z_4)$ are related to the suspension relative travel, and $(z_d - z_{b5})$ is the driver relative bounce.

Changing Eq. (7) into a general matrix format, the optimal matrix will be

$$Q = \begin{bmatrix} ee_1 & 0 & 0 & 0 & e_{15} & e_{16} & e_{17} & 0 & 0 & 0 & 0 & 0 & 0 & 0 & 0 \\ 0 & ee_2 & 0 & 0 & e_{25} & e_{26} & e_{27} & 0 & 0 & 0 & 0 & 0 & 0 & 0 & 0 \\ 0 & 0 & ee_3 & 0 & e_{35} & e_{36} & e_{37} & 0 & 0 & 0 & 0 & 0 & 0 & 0 & 0 \\ 0 & 0 & 0 & ee_4 & e_{45} & e_{46} & e_{47} & 0 & 0 & 0 & 0 & 0 & 0 & 0 & 0 \\ e_{15} & e_{25} & e_{35} & e_{45} & ee_5 & e_{56} & e_{57} & e_{58} & 0 & 0 & 0 & 0 & e_{513} & e_{514} & e_{515} & e_{516} \\ e_{16} & e_{26} & e_{36} & e_{46} & e_{56} & ee_6 & e_{67} & e_{68} & 0 & 0 & 0 & 0 & e_{613} & e_{614} & e_{615} & e_{616} \\ e_{17} & e_{27} & e_{37} & e_{47} & e_{57} & e_{67} & ee_7 & e_{78} & 0 & 0 & 0 & 0 & e_{713} & e_{714} & e_{715} & e_{716} \\ 0 & 0 & 0 & 0 & e_{58} & e_{68} & e_{78} & ee_8 & 0 & 0 & 0 & 0 & e_{813} & e_{814} & e_{815} & e_{816} \\ 0 & 0 & 0 & 0 & 0 & 0 & 0 & 0 & ee_9 & 0 & 0 & 0 & 0 & 0 & 0 & 0 \\ 0 & 0 & 0 & 0 & 0 & 0 & 0 & 0 & 0 & ee_{10} & 0 & 0 & 0 & 0 & 0 & 0 \\ 0 & 0 & 0 & 0 & 0 & 0 & 0 & 0 & 0 & 0 & ee_{11} & 0 & 0 & 0 & 0 & 0 \\ 0 & 0 & 0 & 0 & 0 & 0 & 0 & 0 & 0 & 0 & 0 & ee_{12} & 0 & 0 & 0 & 0 \\ 0 & 0 & 0 & 0 & e_{513} & e_{613} & e_{713} & e_{813} & 0 & 0 & 0 & 0 & ee_{13} & e_{1314} & e_{1315} & e_{1316} \\ 0 & 0 & 0 & 0 & e_{514} & e_{613} & e_{713} & e_{813} & 0 & 0 & 0 & 0 & e_{1314} & ee_{14} & e_{1415} & e_{1416} \\ 0 & 0 & 0 & 0 & e_{515} & e_{613} & e_{713} & e_{813} & 0 & 0 & 0 & 0 & e_{1315} & e_{1415} & ee_{15} & e_{1516} \\ 0 & 0 & 0 & 0 & e_{516} & e_{613} & e_{713} & e_{813} & 0 & 0 & 0 & 0 & e_{1316} & e_{1416} & e_{1516} & ee_{16} \end{bmatrix}$$

$$R = \begin{bmatrix} R_1 & 0 & 0 & 0 & 0 \\ 0 & R_2 & 0 & 0 & 0 \\ 0 & 0 & R_3 & 0 & 0 \\ 0 & 0 & 0 & R_4 & 0 \\ 0 & 0 & 0 & 0 & R_5 \end{bmatrix}$$

Linear optimal control theory [11] provides the controller gain of Eq. (5) using the performance index relation of Eq. (6). This procedure results in the gain matrix k as

$$k = -R^{-1}BP \quad (8)$$

where the matrix P is obtained by solving the algebraic Riccati equation

$$A^T P + PA - PBR^{-1}B^T P + Q = 0 \quad (9)$$

Equation (1) for the optimal closed-loop system may be written in the form

$$\dot{x} = (A - BK)x + Gw \quad (10)$$

Which is the form ultimately used in the simulation performed.

4. Optimal observer design

We have previously assumed that the state vector is available for use in the optimal state feedback law. It might appear that the state feedback method is not applicable in practice, since the whole state is not available. However, it is possible to estimate the states of the system, provided the system is detectable. In order to be able to provide the necessary states used in the feedback law, a reduced order state-space observer is designed to estimate those states that are not directly measurable. It is possible to recover much of the behavior of the state feedback law by using state estimates instead of states in the feedback law.

The input to the state observer is the system output measurement y , which generally could be expressed in the form

$$y = Cx + v \quad (11)$$

where x is the system states and v is the measurement noise. A typical sensor arrangement for passenger cars can provide the relative suspension travel and the relative passenger bounce. For this case we have

$$C = \begin{bmatrix} 1 & 0 & 0 & 0 & -1 & b_2 & a_1 & 0 & 0 & 0 & 0 & 0 & 0 & 0 & 0 & 0 \\ 0 & 1 & 0 & 0 & -1 & -b_1 & a_1 & 0 & 0 & 0 & 0 & 0 & 0 & 0 & 0 & 0 \\ 0 & 0 & 1 & 0 & -1 & b_2 & -a_2 & 0 & 0 & 0 & 0 & 0 & 0 & 0 & 0 & 0 \\ 0 & 0 & 0 & 1 & -1 & -b_1 & -a_2 & 0 & 0 & 0 & 0 & 0 & 0 & 0 & 0 & 0 \\ 0 & 0 & 0 & 0 & 1 & b_d & -a_d & -1 & 0 & 0 & 0 & 0 & 0 & 0 & 0 & 0 \end{bmatrix} \quad (12)$$

The observer structure is in the form of

$$\dot{\hat{x}} = A\hat{x} + Bu + L(y - C\hat{x}) \quad (13)$$

where L is the optimal observer gain matrix that produces an LQG optimal estimate of x , denoted as \hat{x} [6]. The optimal gain matrix L can be evaluated using the relation

$$L = PC^T V^{-1} \quad (14)$$

where P is the positive definite solution of the Riccati equation given by

$$A^T P + PA - PC^T V^{-1} CP + W = 0 \quad (15)$$

In this equation, $W = E[ww^T]$, $V = E[vv^T]$ are the plant distribution and measurement noise covariances and E stands for the usual statistical expectation. Notice that in this equation, \hat{x} is a function of the output y and input u , but the input u itself is generated by a state feedback law as

$$u = -k\hat{x} \quad (16)$$

Therefore, for simulation purposes, we can augment the system dynamic equation (Eq. (1)) with that of the observer (Eq. (13)), and solve the augmented system altogether as illustrated by the following equation.

$$\begin{bmatrix} \dot{x} \\ \dot{\hat{x}} \end{bmatrix} = \begin{bmatrix} A & -BK \\ LC & A - BK - LC \end{bmatrix} \begin{bmatrix} x \\ \hat{x} \end{bmatrix} + \begin{bmatrix} x \\ \hat{x} \end{bmatrix} + \begin{bmatrix} G & 0 \\ 0 & L \end{bmatrix} \begin{bmatrix} w \\ v \end{bmatrix} \quad (17)$$

5. Simulation results

In this section the performance of Kalman optimal observer in estimating system states is demonstrated. Also, the effects of active system to remedy the drawbacks of the passive system are examined. The simulation is done in Matlab 7.1 software.

5.1. Optimal Kalman observer performance

Figure 2 shows the comparison made between the first four system states and their estimations. These states are front right tire bounce, front left tire bounce, rear right tire bounce, and rear left tire bounce. Also, Fig. 4 shows the comparison made between the second four system states and their estimations. These states are body roll, body pitch, body bounce, and driver bounce. To better detect the observer performance, the error related to the observer estimation is shown in Figs 3 and 5. As it is clear in Figs 2 to 5, despite the random input, the estimations are quite close to the true system states and this performance is achieved because the Kalman observer works as an optimal estimator.

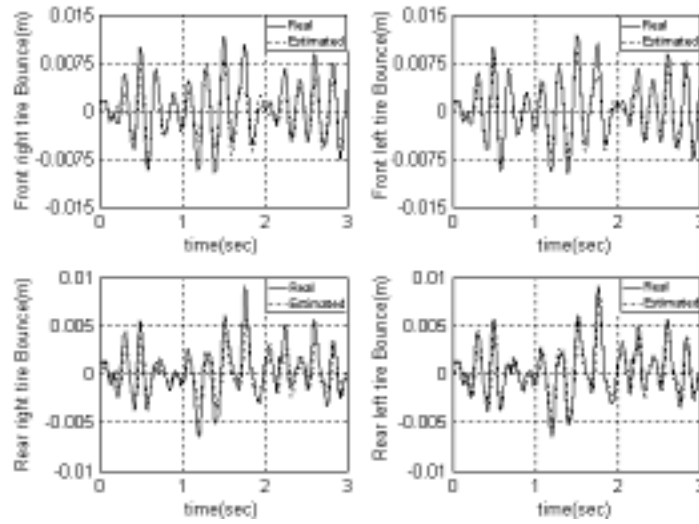


Fig. 2. Comparison of real and estimated states for the front and rear suspension bounces.

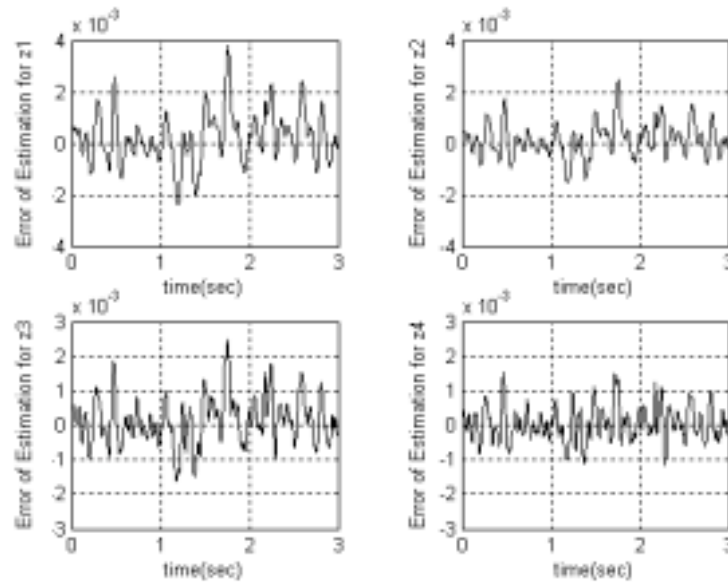


Fig. 3. Error of the estimation for the first four states.

5.2. Comparison between active and passive system states

Figure 6 shows the comparison made between the passive and active system states including front tires bounce, rear tires bounce, body bounce, and driver bounce. Also, in Fig. 7, a comparison made between body pitch and driver acceleration from passive and active systems is presented.

From Fig. 6, it is clear that front and rear tire bounces in the active system are smaller than those of the passive system. Also, body pitch and driver bounce are reduced. In Fig. 7, it can be observed that these two states are reduced considerably.

It is also clear that the tire deflection is a factor of road handling. Moreover, body pitch and driver acceleration are important criteria for the ride comfort. It is therefore concluded that the active system retains better ride comfort characteristics as compared with the passive system.

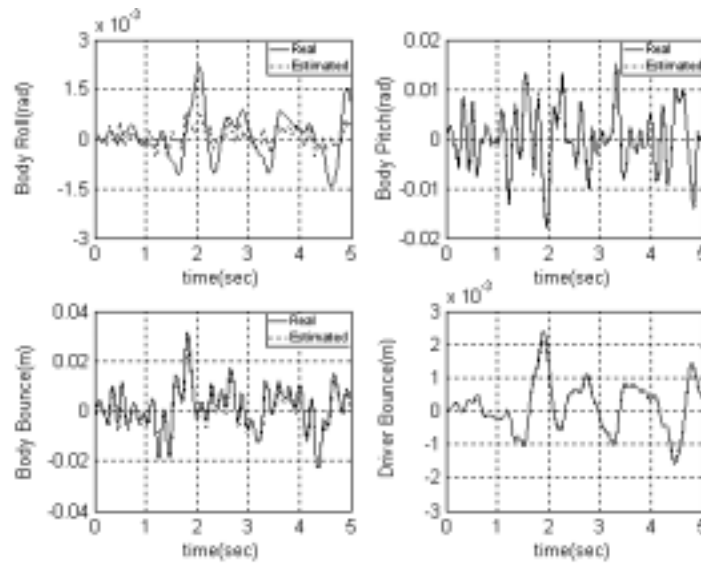


Fig. 4. Comparison of real and estimated states including body roll, body pitch, body bounce, and driver bounce.

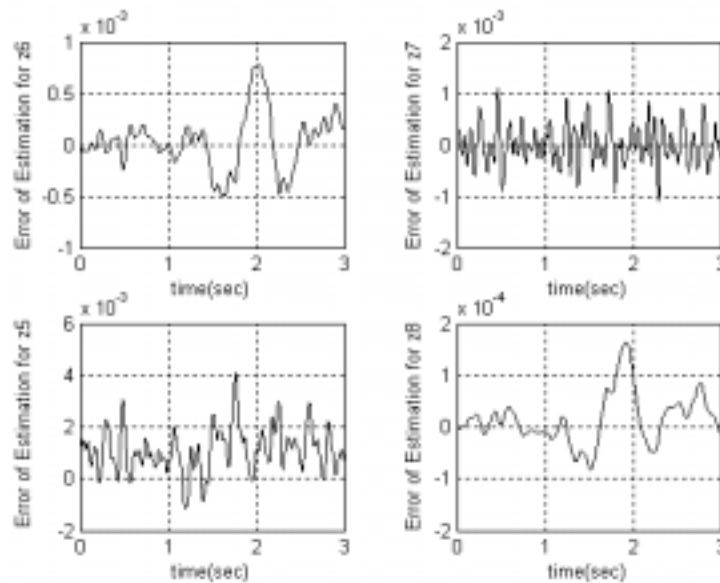


Fig. 5. Error of the estimation for the second four states.

6. Conclusions

The objective of this paper is to examine the use of optimal state-feedback controller to improve the ride comfort in a passenger car. In this paper, the driver seat was included in the full vehicle, so that the response of the driver due to road disturbances can be observed. The potential for improved vehicle ride comfort and road handling that can be achieved from the controlled actuator forces is examined.

The performance characteristics of such a suspension system is evaluated and compared with that of a passive suspension system.

The Kalman observer used to estimate the system unmeasurable states showed a good performance due to the fact that Kalman observer is an optimal estimator in nature.

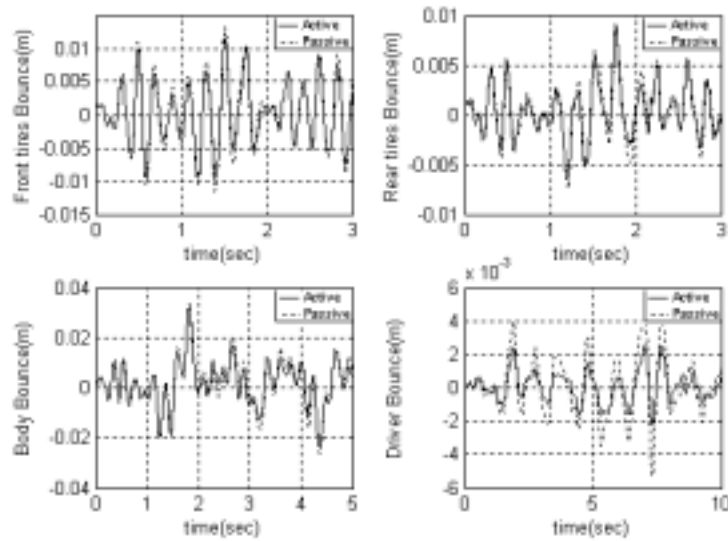


Fig. 6. Comparison between passive and active systems for the front and rear tires bounce, body bounce, and driver bounce.

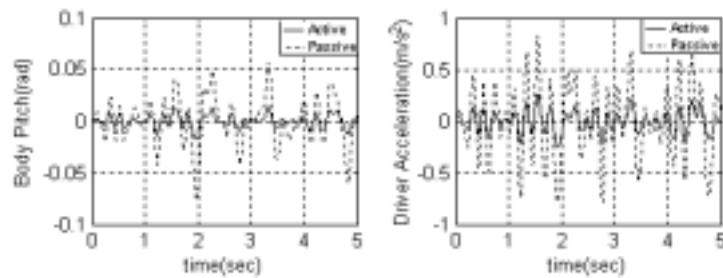


Fig. 7. Comparison between passive and active systems for the body pitch and driver acceleration.

The suspension designs which have emerged from the use of optimal state-feedback control theory proved to be effective in controlling the vehicle vibrations and achieving a better performance as compared with the conventional passive suspension.

Acknowledgment

We would like to express our gratitude to Dr. Shahram Azadi from the Dept. of Mechanical Engineering at the K.N.Toosi University of Technology for his sincere assistance throughout this research work.

Nomenclature and data

The definition of the nomenclature and their actual values taken from a real Samand vehicle is followed in Table 2. This vehicle is considered as the “National Vehicle of Iran” whose manufacture began around 2003.

Table 2
Nomenclature and data

| Not. | Discription | Value |
|----------|----------------------------------|--------------------------|
| I_{xx} | Body inertia around x | 398.4 kg.m ² |
| I_{yy} | Body inertia around y | 1872.4 kg.m ² |
| m_1 | Front right suspension mass | 95 kg |
| m_2 | Front left suspension mass | 95 kg |
| m_3 | Rear left suspension mass | 90 kg |
| m_4 | Rear right suspension mass | 90 kg |
| m_b | Body mass | 1161.9 kg |
| m_d | Passenger mass | 90 kg |
| a_1 | Dimension | 1039.5 mm |
| a_2 | Dimension | 1635.1 mm |
| b_1 | Dimension | 724 mm |
| b_2 | Dimension | 724 mm |
| a_d | Dimension | 650 mm |
| b_d | Dimension | 500 mm |
| k_{fr} | Front right suspension stiffness | 20040 N/m |
| k_{fl} | Front left suspension stiffness | 20040 N/m |
| k_{rl} | Rear left suspension stiffness | 24960 N/m |
| k_{rr} | Rear right suspension stiffness | 24960 N/m |
| k_d | Passenger seat stiffness | 16000 N/m |
| k_{tf} | Front tires stiffness | 177500 N/m |
| k_{tr} | Rear tires stiffness | 177500 N/m |
| k_{ar} | Antiroll bar stiffness | 43000 N/m |
| c_{fr} | Front right damping | 965 Ns/m |
| c_{fl} | Front left damping | 965 Ns/m |
| c_{rl} | Rear left damping | 4000 Ns/m |
| c_{rr} | Rear right damping | 4000 Ns/m |

Appendix A: Equations of motion for the 8-DOF vehicle

Using the Lagrange method, the dynamic equations of motion for the different coordinates of the 8-DOF vehicle have been derived and presented in their final simplified forms here in Appendix A.

Front right tire:

$$m_1\ddot{z}_1 + k_f(z_1 - z_b + b_2\theta_r + a_1\theta_p) - k_{tf}(z_{fr} - z_1) + k_{ar}[(z_1 - z_2)/(b_1 + b_2)^2 + \theta_r/(b_1 + b_2)] + c_f(\dot{z}_1 - \dot{z}_b + b_2\dot{\theta}_r + a_1\dot{\theta}_p) = -u_1 \quad (\text{A1})$$

Front left tire:

$$m_2\ddot{z}_2 + k_f(z_2 - z_b - b_1\theta_r + a_1\theta_p) - k_{tf}(z_{fl} - z_2) - k_{ar}[(z_1 - z_2)/(b_1 + b_2)^2 + \theta_r/(b_1 + b_2)] + c_f(\dot{z}_2 - \dot{z}_b - b_1\dot{\theta}_r + a_1\dot{\theta}_p) = -u_2 \quad (\text{A2})$$

Rear right tire:

$$m_3\ddot{z}_3 + k_r(z_3 - z_b - b_1\theta_r - a_2\theta_p) - k_{tr}(z_{rl} - z_3) + c_r(\dot{z}_3 - \dot{z}_b - b_1\dot{\theta}_r - a_2\dot{\theta}_p) = -u_3 \quad (\text{A3})$$

Rear left tire:

$$m_4\ddot{z}_4 + k_r(z_4 - z_b - a_2\theta_p + b_2\theta_r) - k_{tr}(z_{rr} - z_4) + c_r(\dot{z}_4 - \dot{z}_b - a_2\dot{\theta}_p + b_2\dot{\theta}_r) = -u_4 \quad (\text{A4})$$

Body bounce:

$$m_b\ddot{z}_b - k_f(z_1 - z_b + b_2\theta_r + a_1\theta_p) - k_f(z_2 - z_b - b_1\theta_r + a_1\theta_p) - k_r(z_3 - z_b - b_1\theta_r - a_2\theta_p) - k_r(z_4 - z_b - a_2\theta_p + b_2\theta_r) + k_d(z_b - a_d\theta_p + b_d\theta_r - z_d) - c_f(\dot{z}_1 - \dot{z}_b + b_2\dot{\theta}_r + a_1\dot{\theta}_p) - c_f(\dot{z}_2 - \dot{z}_b - b_1\dot{\theta}_r + a_1\dot{\theta}_p) - c_r(\dot{z}_3 - \dot{z}_b - b_1\dot{\theta}_r - a_2\dot{\theta}_p) - c_r(\dot{z}_4 - \dot{z}_b - a_2\dot{\theta}_p + b_2\dot{\theta}_r) + c_d(\dot{z}_b - a_d\dot{\theta}_p + b_d\dot{\theta}_r - \dot{z}_d) = u_1 + u_2 + u_3 + u_4 - u_5 \quad (\text{A5})$$

Body roll:

$$\begin{aligned} I_{xx}\ddot{\theta}_r + b_2k_f(z_1 - z_b + b_2\theta_r + a_1\theta_p) - b_1k_f(z_2 - z_b - b_1\theta_r + a_1\theta_p) + b_1k_r(z_3 - z_b + b_2\theta_r - a_2\theta_p) \\ - b_1k_r(z_4 - z_b - a_2\theta_p - b_1\theta_r) + b_dk_d(z_b - a_d\theta_p + b_d\theta_r - z_d) + k_{ar}(\theta_r + \frac{z_1 - z_2}{b_1 + b_2}) \\ + b_2c_f(\dot{z}_1 - \dot{z}_b + b_2\dot{\theta}_r + a_1\dot{\theta}_p) - b_1c_f(\dot{z}_2 - \dot{z}_b - b_1\dot{\theta}_r + a_1\dot{\theta}_p) - b_2c_r(\dot{z}_3 - \dot{z}_b + b_2\dot{\theta}_r - a_2\dot{\theta}_p) \\ - b_1c_r(\dot{z}_4 - \dot{z}_b - b_1\dot{\theta}_r + a_2\dot{\theta}_r) + b_dc_d(\dot{z}_b - a_d\dot{\theta}_p + b_d\dot{\theta}_r - \dot{z}_d) = -b_2u_1 + b_1u_2 - b_2u_3 + b_1u_4 - b_du_5 \end{aligned} \quad (A6)$$

Body pitch:

$$\begin{aligned} I_{yy}\ddot{\theta}_p + a_1k_f(z_1 - z_b + b_2\theta_r + a_1\theta_p) + a_1k_f(z_2 - z_b - b_1\theta_r + a_1\theta_p) - a_2k_r(z_3 - z_b - b_1\theta_r - a_2\theta_p) \\ - a_2k_r(z_4 - z_b - a_2\theta_p + b_2\theta_r) - a_dk_d(z_b - a_d\theta_p + b_d\theta_r - z_d) + a_1c_f(\dot{z}_1 - \dot{z}_b + b_2\dot{\theta}_r + a_1\dot{\theta}_p) \\ + a_1c_f(\dot{z}_2 - \dot{z}_b - b_1\dot{\theta}_r + a_1\dot{\theta}_p) - a_2c_r(\dot{z}_3 - \dot{z}_b - b_1\dot{\theta}_r - a_2\dot{\theta}_p) - a_2c_r(\dot{z}_4 - \dot{z}_b - a_2\dot{\theta}_p + b_2\dot{\theta}_r) \\ - a_dc_d(\dot{z}_b - a_d\dot{\theta}_p + b_d\dot{\theta}_r - \dot{z}_d) = -a_1u_1 - a_1u_2 + a_2u_3 + a_2u_4 + a_du_5 \end{aligned} \quad (A7)$$

Driver bounce:

$$m_d\ddot{z}_d - k_d(z_b - a_d\theta_p + b_d\theta_r - z_d) + c_d(\dot{z}_b - a_d\dot{\theta}_p + b_d\dot{\theta}_r - \dot{z}_d) = u_5 \quad (A8)$$

Appendix B: The elements of the Q matrix used in the optimal control method

$$\begin{aligned} r_5 &= A(16, 5), r_6 = A(16, 6), r_7 = A(16, 7), r_8 = A(16, 8), r_{13} = A(16, 13), \\ r_{14} &= A(16, 14), r_{15} = A(16, 15), r_{16} = A(16, 16), r_d = 1/m_d \\ ee_1 &= q_1, ee_2 = q_2, ee_3 = q_3, ee_4 = q_4, ee_5 = q_1 + q_2 + q_3 + q_4 + q_5 + r_5^2 \cdot q_7 \\ ee_6 &= b_2^2q_1 + b_1^2q_2 + b_2^2q_3 + b_1^2q_4 + b_2^2q_5 + r_6^2 \cdot q_7 \\ ee_7 &= a_1^2q_1 + a_2^2q_2 + a_2^2q_3 + a_2^2q_4 + a_d^2q_5 + q_6 + r_6^2 \cdot q_7 \\ ee_8 &= q_5 + r_8^2 \cdot q_7, ee_{13} = r_{13}^2 \cdot q_7, ee_{14} = r_{14}^2 \cdot q_7, ee_{15} = r_{15}^2 \cdot q_7, ee_{16} = r_{16}^2 \cdot q_7 \\ e_{15} &= -q_1, e_{16} = b_2q_1, e_{17} = a_1q_1, e_{25} = -q_2, e_{26} = -b_1q_2, e_{27} = a_1q_2 \\ e_{35} &= -q_3, e_{36} = b_2q_3, e_{37} = -a_2q_3, e_{45} = -q_4, e_{46} = -b_1q_4, e_{47} = -a_2q_4 \\ e_{56} &= -b_2q_1 + b_1q_2 - b_2q_3 + b_1q_4 + b_dq_5 + r_5 \cdot r_6 \cdot q_7, e_{57} = -a_1q_1 - a_1q_2 + a_2q_3 + a_2q_4 + a_dq_5 + r_5 \cdot r_7 \cdot q_7 \\ e_{58} &= -q_5 + r_5 \cdot r_8 \cdot q_7, e_{513} = r_5 \cdot r_{13} \cdot q_7, e_{514} = r_5 \cdot r_{14} \cdot q_7, e_{515} = r_5 \cdot r_{15} \cdot q_7, e_{516} = r_5 \cdot r_{16} \cdot q_7 \\ e_{67} &= a_1b_2q_1 - a_1b_1q_2 + a_2b_2q_3 + a_2b_1q_4 - a_db_dq_5 + r_6 \cdot r_7 \cdot q_7 \\ e_{68} &= -b_dq_5 + r_6 \cdot r_8 \cdot q_7, e_{613} = r_6 \cdot r_{13} \cdot q_7, e_{614} = r_6 \cdot r_{14} \cdot q_7, e_{615} = r_6 \cdot r_{15} \cdot q_7, e_{616} = r_6 \cdot r_{16} \cdot q_7, \\ e_{78} &= a_dq_5 + r_7 \cdot r_8 \cdot q_7, e_{713} = r_7 \cdot r_{13} \cdot q_7, e_{714} = r_7 \cdot r_{14} \cdot q_7, e_{715} = r_7 \cdot r_{15} \cdot q_7, e_{716} = r_7 \cdot r_{16} \cdot q_7, \\ e_{813} &= r_8 \cdot r_{13} \cdot q_7, e_{814} = r_8 \cdot r_{14} \cdot q_7, e_{815} = r_8 \cdot r_{15} \cdot q_7, e_{816} = r_8 \cdot r_{16} \cdot q_7 \\ e_{1314} &= r_{13} \cdot r_{14} \cdot q_7, e_{1315} = r_{13} \cdot r_{15} \cdot q_7, e_{1316} = r_{13} \cdot r_{16} \cdot q_7 \\ e_{1415} &= r_{13} \cdot r_{15} \cdot q_7, e_{1416} = r_{13} \cdot r_{16} \cdot q_7, e_{1516} = r_{13} \cdot r_{14} \cdot q_7 \end{aligned}$$

References

- [1] S. Malekzadeh, *Analytical Scrutiny and Computer Simulation of Vehicle in Response to road Ramps*, B.S. Thesis, Tabriz University, Tabriz, Iran, 2004.
- [2] K. Hyo-Jun, S.H. Yang and P. Young-Pil, Improving the vehicle performance with active suspension using road-sensing algorithm, *Elsevier, Computers and Structures* (2002), 80-1569–1577.
- [3] K. Jeong-Hoon and L. Chong-Won, Semi-active damping control of suspension systems for specified operational response mode, *Journal of Sound and Vibration* **260** (2003), 307–328.
- [4] T.D. Gillespie, *Fundamentals of vehicle Dynamics*, SAE Inc, 1992.
- [5] H.D. Taghirad and E. Esmailzadeh, *Passenger ride comfort through observer based control*, In proceeding of the 15th ASME biennial conference on Mechanical Vibration and Noise, 1995.
- [6] F. Yu, J.-W. Zhang and D.A. Crolla, A study of kalman filter active vehicle suspension system using correlation of front and rear wheel road inputs, *Proceeding institute Mechanical Engineering* **214** (2000), part D.
- [7] T.J. Gordon and R.S. Sharp, On Improving the performance of automotive semi-active suspension systems through road preview, *Journal of Sound and Vibration* **217**(1) (1998), 163–182.

- [8] Y.J. Li, Optimal preview control design of active and semi-active suspension systems including jerk, *society of automotive engineers*, Inc, 1996.
- [9] R.A. Williams, Automotive active suspensions-Part 1:Basic principles, Engineering center, Jaguar Cars, Coventry, *Proceeding institute Mechanical Engineering* **211** (1997), part D.
- [10] R.G.M. Huisman, An optimal continuous-time control strategy for active suspensions with preview, *Journal of Vehicle System Dynamics* **22** (1993), 43–55.
- [11] J.B. Burl, *Linear Optimal Control*, Michigan Technological University, 1998.
- [12] T.E. Fortman and K.L. Hitz, *An Introduction to Linear Control Systems*, Marcel Dekker, New York, 1997.



Hindawi

Submit your manuscripts at
<http://www.hindawi.com>

